Predictive Coding of Bit Loading for Time-Correlated MIMO Channels With a Decision Feedback Receiver

Chien-Chang Li and Yuan-Pei Lin, *Senior Member, IEEE*

***Abstract*—In this paper, we consider variable-rate transmission over a slowly varying multiple-input multiple-output (MIMO) channel with a decision feedback receiver. The transmission rate is adapted to the channel by dynamically assigning bits to the subchannels of the MIMO system. Predictive quantization is used for the feedback of bit loading to take advantage of the time correlation inherited from the temporally correlated channel. Due to the use of decision feedback at the receiver, the bit loading is related to the Cholesky decomposition of the channel Gram matrix. Assuming the channel is modeled by a slowly varying Gauss–Markov process, we show that the nested submatrices generated during the process of Cholesky decomposition can be updated as time evolves. Based on the update, we derive the optimal predictor of the next bit loading for predictive quantization. Furthermore, we derive the statistics of the prediction error, which are then exploited to design the quantizer to achieve a smaller quantization error. Simulations are given to demonstrate that the proposed predictive quantization gives a good approximation of the desired transmission rate with a low feedback rate.**

***Index Terms*—MIMO, limited feedback, differential feedback, predictive quantization, bit loading, variable rate transmission.**

I. Introduction

MULTIPLE-INPUT multiple-output (MIMO) systems have attracted great attention in recent years. Optimal precoders of different design criteria for MIMO channels have been considered in [1]–[4] for a fixed transmission rate. To increase the transmission rate over a fading channel, variable-rate transmission systems are proposed in [5]–[9]. Adapting the transmission rate according to the channel also has the advantage that the error rate can be easily controlled without deep interleaving. In [1]–[9], the channel state information (CSI) are assumed to be available to both the transmitter and receiver. In general, the transmitter has no complete CSI and there is only limited amount of feedback [10]. Depending on the transmission scheme, the receiver feeds back the information of the precoder, power loading, bit loading, or channel Gram matrix to the transmitter [11]–[18]. Precoder codebooks for a fixed bit loading are designed in [11]–[15]. The feedback of power loading and antenna rate control is proposed in [16], [17]. Bit loading codebooks for a given precoder are designed in [18]. In these works, the channel is assumed to be independent of time.

In practical transmission, the channel is usually correlated in time. Time-correlated channels have been considered in [19]–[25]. In [19], the precoder is fed back to the transmitter using Givens rotations for correlated MIMO channels. In [20], the channel Gram matrix is differentially coded using geodesic curves and a differential codebook is designed for maximizing the signal to noise ratio or mutual information. In [21], a beamforming system with limited feedback is designed by modeling the quantized CSI as a finite state Markov chain. In [22]–[25], a temporally correlated channel is modeled as a first-order Gauss-Markov process. The channel capacity for such a channel is analyzed in [22]. A rotation based differential codebook for the precoding matrix is proposed in [23]. In [24], the minimum feedback rate for a differential feedback system is derived in a closed-form. A polar-cap differential codebook is proposed in [25] for a beamforming system with limited feedback. In [26], predictive quantization was applied on the feedback of bit loading for a linear receiver, and the quantizer was designed using the bounds of the prediction error variance.

In this paper, we consider variable-rate transmission for a slowly time-varying MIMO channel when decision feedback is used at the receiver. The full channel information is assumed to be available at the receiver. The transmitter does not know the channel information $\mathbf{H}_n$. The information that is available to the transmitter is the feedback from the receiver. For a given error rate constraint, bits are dynamically assigned to each subchannel according to the channel information as in per-antenna rate control (PARC) [16] so that the transmission rate can be adapted to the current channel. Due to the temporal correlation of the channel, the bit loading is also time correlated. We feedback the bit loading vector using predictive quantization as in [26] assuming a delay free feedback loop is available. When decision feedback is employed at the receiver with reverse detection order, it is known that the Cholesky decomposition of the channel Gram matrix can be used to determine the subchannel signal-to-noise ratios and hence also the bit loading. Assuming the time correlated channel is modeled by a slowly varying Gauss-Markov process, we show that the submatrices generated during the process of Cholesky decomposition can be updated with time. The update allows us to obtain the optimal predictor of the next bit loading for predictive quantization in a closed form. Furthermore, we analyze the statistics of the subchannel prediction errors and derive their means and variances. The statistics are then exploited in the design of quantizers for

Manuscript received February 07, 2014; revised August 31, 2014 and December 23, 2014; accepted March 23, 2015. Date of publication April 10, 2015; date of current version May 29, 2015. The associate editor coordinating the review of this manuscript and approving it for publication was Prof. Urbashi Mitra. This work was supported in parts by National Science Council, Taiwan, R. O. C., under NSC 101-2221-E-009-091-MY3 and Aiming for the Top University Plan of National Chiao-Tung University, the Ministry of Education, Taiwan, under Contract 100W9633 and 101W963.

C.-C. Li is with the Office of Chief Technology Officer, MediaTek Inc., Hsinchu Science Park, Hsinchu, Taiwan 300 (e-mail: ecehalliday@gmail.com).

Y.-P. Lin is with the Department of Electrical Engineering, National Chiao Tung University, Taiwan 300 (e-mail: ypl@mail.nctu.edu.tw).

Digital Object Identifier 10.1109/TSP.2015.2421471

quantizing the prediction errors. By adapting the quantizers according to the statistics of the prediction errors, a smaller quantization error than direct quantization can be achieved. Simulations are given to demonstrate that for slowly varying channels, the proposed predictive quantization of bit loading can achieve a rate very close to the unquantized case with a low feedback rate.

The rest of the paper is organized as follows. In Section II, we introduce the system model of the time-varying MIMO system and give an overview of the proposed predictive quantization of bit loading. In Section III, we derive the update of the submatrices associated with the Cholesky decomposition of the channel Gram matrix. Using the results in the update of the Cholesky decomposition, we derive the predictor of bit loading in Section IV. The statistics of the predictive errors are analyzed and exploited to adapt the quantizers in Section V. In Section VI, we demonstrate the performance of the proposed system by simulations.

II. System Model

A MIMO communication system with a decision feedback receiver is shown in Fig. 1. At time n, the MIMO channel is modeled by an $M_r \times M_t$ matrix $\mathbf{H}_n$. The elements of $\mathbf{H}_n$ are i.i.d. circularly symmetric complex Gaussian random variables with unit variance. We assume the channel is a first-order Gauss-Markov process [22],

$$\mathbf{H}_{n+1} = \sqrt{1-\epsilon^2}\mathbf{H}_n + \epsilon \mathbf{W}_n, \tag{1}$$

where ϵ is a coefficient that depends on the doppler frequency. When the Jake's model [27] is used, $\epsilon = \sqrt{1-(J_0(2\pi f_d T_s))^2}$, where $J_0(\cdot)$ is the zeroth order Bessel function of the first kind, f_d is the maximum Doppler frequency, T_s is the time interval between consecutive channel uses. The $M_r \times M_t$ matrix $\mathbf{W}_n$ is independent of $\mathbf{H}_n$ and its elements are identical and independent circularly symmetric complex Gaussian random variables with unit variance. We assume $M_r \geq M_t$ and the number of substreams transmitted is $\min(M_r, M_t) = M_t$. The case $M_r < M_t$ is addressed in Section V. The input of the transmitter $\mathbf{s}_n$ is an $M_t \times 1$ vector of uncorrelated modulation symbols $s_{n,1}, s_{n,2}, \ldots, s_{n,M_t}$. We assume the symbols are of zero mean and variance P_0/M_t, where P_0 is the total transmit power. The $M_r \times 1$ channel noise $\mathbf{q}_n$ is additive white complex Gaussian noise with zero mean and variance N_0. $\mathbf{G}_n$ is the feedforward matrix of size $M_t \times M_r$ and $\mathbf{B}_n$ is the feedback matrix of size $M_t \times M_t$. The input of the receiver is given by $\mathbf{y}_n = \mathbf{H}_n\mathbf{s}_n + \mathbf{q}_n$. Let $\mathbf{z}_n$ be the input to the detector. $\mathbf{z}_n$ can be expressed as $\mathbf{z}_n = \mathbf{G}_n\mathbf{y}_n - \mathbf{B}_n\widehat{\mathbf{s}}_n$. When reverse detection ordering is used, the feedforward matrix $\mathbf{G}_n$ and the feedback matrix $\mathbf{B}_n$ can be given in terms of the QR decomposition of the channel [28]. Let the QR decomposition of $\mathbf{H}_n$ be $\mathbf{Q}_n\mathbf{R}_n$, where $\mathbf{Q}_n$ is an $M_r \times M_t$ matrix with orthonormal columns and $\mathbf{R}_n$ is an $M_t \times M_t$ upper triangular matrix with the (i, j)th element denoted as $r_{n,ij}$. Then $\mathbf{G}_n$ and $\mathbf{B}_n$ are given, respectively, by [28]

$$\begin{aligned}\mathbf{G}_n &= \mathrm{diag}\{\, r_{n,11}^{-1} \quad r_{n,22}^{-1} \quad \cdots \quad r_{n,M_tM_t}^{-1} \,\}\mathbf{Q}_n^{\dagger}, \\ \mathbf{B}_n &= \mathrm{diag}\{\, r_{n,11}^{-1} \quad r_{n,22}^{-1} \quad \cdots \quad r_{n,M_tM_t}^{-1} \,\}\mathbf{R}_n - \mathbf{I}_{M_t}, \end{aligned} \tag{2}$$

where $\dagger$ denotes the transpose conjugate and the notation $\mathbf{I}_{M_t}$ is used to represent the $M_t \times M_t$ identity matrix. Define the kth subchannel error as $e_{n,k} = s_{n,k} - \hat{s}_{n,k}$. Assuming there is no error propagation, using (2) the subchannel error $e_{n,k}$ has variance given by

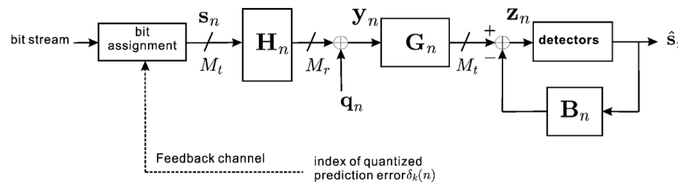

Fig. 1. MIMO system with decision feedback receiver.

$$\sigma_{e_{n,k}}^2 = N_0 r_{n,kk}^{-2}, \tag{3}$$

for $k = 1, 2, \ldots, M_t$. Suppose the target symbol error rate of the kth subchannel is ξ_k. The number of bits that can be loaded on the k-th subchannel at time n is well approximated by [29]

$$b_{n,k} = \log_2(1 + \gamma_k r_{n,kk}^2), \tag{4}$$

where $\gamma_k = P_0/(\Gamma_k M_t N_0)$. Γ_k is the so-called SNR gap, given by $\Gamma_k = [Q^{-1}(\xi_k/4)]^2/3$ [30]. The function $Q(x)$ is the area under a Gaussian tail, i.e., $Q(x) = (1/\sqrt{2\pi})\int_x^{\infty} e^{-u^2/2}du$. Define the bit loading vector at time n as $\mathbf{b}_n = [\, b_{n,1} \quad b_{n,2} \quad \cdots \quad b_{n,M_t} \,]^T$. In this paper, we consider the feedback of bit loading vector in a slowly time-varying MIMO channel using predictive quantization, assuming a delay-free feedback loop is available. Note that $b_{n,k}$, a positive real number as given in (4), is a function of $SNR_{n,k} = P_0 r_{n,kk}^2/(\Gamma_k M_t N_0)$. Thus feedback of the non-integer $b_{n,k}$ is equivalent to feedback of $SNR_{n,k}$. The channel information is assumed to be available at the receiver, i.e., the channel $\mathbf{H}_n$ is known at the receiver at time n. The transmitter does not know the channel $\mathbf{H}_n$. The information that is available at the transmitter is the feedback from the receiver in addition to the transmit power P_0, noise variance N_0, and SNR gap Γ_k. An overview of predictive coding of bit loading is given below.

A. Predictive Quantization of Bit Loading (PQB)

At time $n+1$, both the transmitter and receiver compute a predictor $\widetilde{\mathbf{b}}_{n+1}$ of the bit loading at time $n+1$, using the quantized bit loading $\widehat{\mathbf{b}}_n$ of time n that is available to both the transmitter and receiver. Then the receiver computes the prediction error $\boldsymbol{\delta}_{n+1} = \mathbf{b}_{n+1} - \widetilde{\mathbf{b}}_{n+1}$, quantizes it to $\widehat{\boldsymbol{\delta}}_{n+1}$, and sends $\widehat{\boldsymbol{\delta}}_{n+1}$ back to the transmitter. The transmitter reconstructs the quantized bit loading using

$$\widehat{\mathbf{b}}_{n+1} = \widehat{\boldsymbol{\delta}}_{n+1} + \widetilde{\mathbf{b}}_{n+1}. \tag{5}$$

In this case, the quantization error of bit loading $\mathbf{b}_{n+1} - \widehat{\mathbf{b}}_{n+1}$ is exactly the same as $\boldsymbol{\delta}_{n+1} - \widehat{\boldsymbol{\delta}}_{n+1}$, the quantization error of the prediction error. With proper design of the predictor $\widetilde{\mathbf{b}}_{n+1}$, the prediction error $\boldsymbol{\delta}_{n+1}$ has a smaller variance than $\mathbf{b}_{n+1}$. As quantization error is in general proportional to the variance of the signal to be quantized [31], predictive quantization can achieve a smaller quantization error than direct quantization. Note that the bit loading $b_{n,k}$ in (4) is not an integer in general, and neither is the quantized bit loading $\widehat{b}_{n,k}$. To obtain integer bit loading, we can truncate $\widehat{b}_{n,k}$ to the nearest integer. The number of bits that is actually loaded on the kth subchannel at time n is $\lfloor \widehat{b}_{n,k} \rfloor$, where the notation $\lfloor x \rfloor$ denotes the largest integer that is less than or equal to x. As a result, each symbol $s_{n,k}$ is drawn from a $2^{\lfloor \widehat{b}_{n,k} \rfloor}$-ary constellation. In [26], predictive coding was also used for quantizing bit loading, but there are some important differences. The receiver in [26] is linear rather than a decision feedback receiver. In this paper, the optimal predictor is obtained using the Cholesky decomposition of the channel Gram matrix, and the prediction error is approximated in a closed form. In [26], only the upper and lower bounds of the optimal predictor and prediction error are given, but explicit formulations are not available.

In the proposed predictive quantization of bit loading, there are two issues to be addressed. One is how to design the predictor $\widetilde{\mathbf{b}}_{n+1}$ so that the prediction error is minimized, and the other is how to quantize the prediction error $\boldsymbol{\delta}_{n+1}$. From (4), we know that the bit loading $\mathbf{b}_n$ is determined by $\{r^2_{n,kk}\}_{k=1}^{M_t}$. It is known that $r^2_{n,kk}$ is closely related to the Cholesky decomposition of the channel Gram matrix $\mathbf{H}_n^\dagger \mathbf{H}_n$. In the next section, we develop an update of the Cholesky decomposition, based on which the optimal predictor is derived in Section IV. The second issue, i.e., quantization of the prediction error, is addressed in Section V.

III. Update of Cholesky Decomposition

In this section, we look into the Cholesky decomposition of $\mathbf{H}_n^\dagger \mathbf{H}_n$ when the channel is modeled by the first-order Gauss-Markov process in (1). We show that the nested submatrices generated in the process of the Cholesky decomposition can be updated in a closed form. The results are used in later sections to derive the prediction of bit loading.

Let the Cholesky decomposition of $\mathbf{H}_n^\dagger \mathbf{H}_n$ be $\mathbf{L}_n \mathbf{D}_n \mathbf{L}_n^\dagger$, where $\mathbf{D}_n$ is an $M_t \times M_t$ diagonal matrix with diagonal element $d_{n,k}$ and $\mathbf{L}_n$ is an $M_t \times M_t$ unit lower triangular matrix [32]. Then we have $d_{n,k} = r^2_{n,kk}$. To obtain the Cholesky decomposition, let us introduce the outer product Cholesky procedure [32]. Define $\mathbf{T}_n^{(1)} = \mathbf{H}_n^\dagger \mathbf{H}_n$ and decompose $\mathbf{T}_n^{(1)}$ as

$$\mathbf{T}_n^{(1)} = \begin{bmatrix} d_{n,1} & \boldsymbol{\ell}_n^{(1)\dagger} \\ \boldsymbol{\ell}_n^{(1)} & \boldsymbol{\Phi}_n^{(1)} \end{bmatrix} \tag{6}$$

$$= \begin{bmatrix} 1 & \mathbf{0} \\ \boldsymbol{\ell}_n^{(1)}/d_{n,1} & \mathbf{I}_{M_t-1} \end{bmatrix} \begin{bmatrix} d_{n,1} & \mathbf{0} \\ \mathbf{0} & \mathbf{T}_n^{(2)} \end{bmatrix} \begin{bmatrix} 1 & \boldsymbol{\ell}_n^{(1)\dagger}/d_{n,1} \\ \mathbf{0} & \mathbf{I}_{M_t-1} \end{bmatrix}, \tag{7}$$

where $\boldsymbol{\ell}_n^{(1)}$ is an $(M_t-1)\times 1$ vector, $\boldsymbol{\Phi}_n^{(1)}$ is an $(M_t-1)\times(M_t-1)$ submatrix, and $\mathbf{T}_n^{(2)} = \boldsymbol{\Phi}_n^{(1)} - \boldsymbol{\ell}_n^{(1)}\boldsymbol{\ell}_n^{(1)\dagger}/d_{n,1}$. Thus, $d_{n,1} = [\mathbf{T}_n^{(1)}]_{11}$, where the notation $[\mathbf{X}]_{kl}$ denotes the $(k,\ l)$th element of a matrix $\mathbf{X}$. Repeating the same procedure, we have

$$\mathbf{T}_n^{(k)} = \boldsymbol{\Phi}_n^{(k-1)} - \boldsymbol{\ell}_n^{(k-1)}\boldsymbol{\ell}_n^{(k-1)\dagger}/d_{n,k-1}, \tag{8}$$

where $\boldsymbol{\ell}_n^{(k-1)}$ is an $(M_t-k+1)\times 1$ vector and $\boldsymbol{\Phi}_n^{(k-1)}$ is the $(M_t-k+1)\times(M_t-k+1)$ submatrix of $\mathbf{T}_n^{(k-1)}$ obtained by removing the first column and the first row. Then $d_{n,k}$ can be obtained by

$$d_{n,k} = [\mathbf{T}_n^{(k)}]_{11}, \ \text{ for } k = 2,3,\ldots,M_t, \tag{9}$$

and the lower triangular matrix $\mathbf{L}_n$ is given by

$$\mathbf{L}_n = \begin{bmatrix} 1 & 0 & \cdots & & 0 \\ & 1 & & & \\ \tilde{\boldsymbol{\ell}}_n^{(1)} & & \ddots & 0 & \vdots \\ & \tilde{\boldsymbol{\ell}}_n^{(2)} & & 1 & 0 \\ & & & \tilde{\boldsymbol{\ell}}_n^{(M_t-1)} & 1 \end{bmatrix},$$

where $\tilde{\boldsymbol{\ell}}_n^{(k)} = \boldsymbol{\ell}_n^{(k)}/d_{n,k}$. In Lemma 1, we show that $\mathbf{T}_n^{(k)}$ is actually the Gram matrix of an appropriately defined reduced channel matrix.

Lemma 1: The matrix $\mathbf{T}_n^{(k)}$ defined in (8) in the outer product Cholesky procedure can be decomposed as

$$\mathbf{T}_n^{(k)} = \mathbf{H}_n^{(k)\dagger}\mathbf{H}_n^{(k)}, \ \text{ for } k = 1,2,\ldots,M_t. \tag{10}$$

where $\mathbf{H}_n^{(1)} = \mathbf{H}_n$, and for $k = 2,3,\ldots,M_t$, the $M_r \times (M_t-k+1)$ matrix $\mathbf{H}_n^{(k)}$ is given by

$$\mathbf{H}_n^{(k)} = \mathbf{H}_n^{(k-1)} \begin{bmatrix} -\tilde{\boldsymbol{\ell}}_n^{(k-1)\dagger} \\ \mathbf{I}_{M_t-k+1} \end{bmatrix}. \tag{11}$$

Furthermore, each column of $\mathbf{H}_n^{(k)}$ is orthogonal to the first column of $\mathbf{H}_n^{(k-1)}$ for $k \geq 2$.

Proof: See Appendix A.

Observe from (11) that $\mathbf{H}_n^{(k)}$ $(k \geq 2)$ can be obtained from $\mathbf{H}_n^{(k-1)}$ as follows. Compute the orthogonal projection of the first column vector of $\mathbf{H}_n^{(k-1)}$ on each of the remaining columns, subtract the orthogonal projection vectors from the respective columns, and remove the first column. Then the resulting matrix is $\mathbf{H}_n^{(k)}$. Therefore, $\mathbf{T}_n^{(k)}$ is actually the Gram matrix of the reduced channel matrix $\mathbf{H}_n^{(k)}$. In Lemma 2, we show that $\mathbf{T}_{n+1}^{(k)}$ can be approximated in terms of $\mathbf{T}_n^{(k)}$.

Lemma 2: Consider the Gauss-Markov channel model in (1) with a small ϵ. Then $\mathbf{T}_{n+1}^{(k)}$ in the outer product Cholesky procedure can be approximated in terms of $\mathbf{T}_n^{(k)}$ as

$$\mathbf{T}_{n+1}^{(k)} \approx \mathbf{T}_n^{(k)} + \epsilon \mathbf{C}_n^{(k)} + \epsilon^2(\mathbf{P}_n^{(k)} - \mathbf{T}_n^{(k)}), \ \text{ for } k=1,2,\ldots,M_t, \tag{12}$$

where the $(M_t-k+1)\times(M_t-k+1)$ matrix $\mathbf{C}_n^{(k)}$ is given by

$$\mathbf{C}_n^{(k)} = \mathbf{H}_n^{(k)\dagger}\mathbf{W}_n^{(k)} + \mathbf{W}_n^{(k)\dagger}\mathbf{H}_n^{(k)}, \tag{13}$$

the $M_r \times (M_t-k+1)$ matrix $\mathbf{W}_n^{(k)}$ is given by $\mathbf{W}_n^{(k)} = \mathbf{W}_n^{(k-1)} \begin{bmatrix} -\tilde{\boldsymbol{\ell}}_n^{(k-1)\dagger} \\ \mathbf{I}_{M_t-k+1} \end{bmatrix}$ for $k = 2,3,\ldots,M_t$, and $\mathbf{W}_n^{(1)} = \mathbf{W}_n$. The $(M_t-k+1)\times(M_t-k+1)$ matrix $\mathbf{P}_n^{(k)}$ is given by

$$\mathbf{P}_n^{(k)} = \mathbf{W}_n^{(k)\dagger}\mathbf{W}_n^{(k)} - \sum_{m=1}^{k-1}(1/d_{n,m})(\mathbf{a}_n^{(m)\dagger}\mathbf{H}_n^{(k)} + \mathbf{v}_n^{(m)\dagger}\mathbf{W}_n^{(k)})^\dagger(\mathbf{a}_n^{(m)\dagger}\mathbf{H}_n^{(k)} + \mathbf{v}_n^{(m)\dagger}\mathbf{W}_n^{(k)}), \tag{14}$$

where the vectors $\mathbf{a}_n^{(m)}$ and $\mathbf{v}_n^{(m)}$ are, respectively, the first columns of $\mathbf{W}_n^{(m)}$ and $\mathbf{H}_n^{(m)}$.

Furthermore, $d_{n+1,k}$ can be approximated in terms of $d_{n,k}$ as

$$d_{n+1,k} \approx d_{n,k} + \epsilon[\mathbf{C}_n^{(k)}]_{11} + \epsilon^2([\mathbf{P}_n^{(k)}]_{11} - d_{n,k}), \ \text{ for } k = 1,2,\ldots,M_t. \tag{15}$$

Proof: See Appendix B.

In the next section, we use the results in Lemma 1 and Lemma 2 to derive the optimal predictor of the next bit loading based on the current bit loading.

IV. Optimal Predictor of Bit Loading Vector

In this section, we derive the optimal predictor $\widetilde{\mathbf{b}}_{n+1}$ of the bit loading vector $\mathbf{b}_{n+1}$ at time $n+1$ given the bit loading vector at time n. Using $d_{n+1,k} = r^2_{n+1,kk}$ and substituting (15) into (4), we have

$$b_{n+1,k} \approx \log_2\left(1+\gamma_k d_{n,k} + \epsilon\gamma_k[\mathbf{C}_n^{(k)}]_{11} + \epsilon^2\gamma_k([\mathbf{P}_n^{(k)}]_{11} - d_{n,k})\right). \quad (16)$$

Using the second order Taylor approximation at $\epsilon = 0$, i.e., $\log_2(1+a\epsilon+b\epsilon^2) \approx \frac{1}{\log_e(2)}\left(a\epsilon + (b-a^2/2)\epsilon^2\right)$, we can verify that

$$b_{n+1,k} \approx b_{n,k} + \frac{1}{\log_e(2)} \cdot \left[\epsilon\frac{[\mathbf{C}_n^{(k)}]_{11}}{\gamma_k^{-1}+d_{n,k}} + \epsilon^2\left(\frac{[\mathbf{P}_n^{(k)}]_{11}-d_{n,k}}{\gamma_k^{-1}+d_{n,k}} - \frac{[\mathbf{C}_n^{(k)}]_{11}^2}{2(\gamma_k^{-1}+d_{n,k})^2}\right)\right]. \quad (17)$$

From (17), we can see that $b_{n+1,k}$ is a function of $[\mathbf{C}_n^{(k)}]_{11}$ and $[\mathbf{P}_n^{(k)}]_{11}$, which depend on $\mathbf{W}_n$ and $\mathbf{H}_n$. Using (13) and (14), $[\mathbf{C}_n^{(k)}]_{11}$ and $[\mathbf{P}_n^{(k)}]_{11}$ are given, respectively, by

$$[\mathbf{C}_n^{(k)}]_{11} = \mathbf{a}_n^{(k)\dagger}\mathbf{v}_n^{(k)} + \mathbf{v}_n^{(k)\dagger}\mathbf{a}_n^{(k)} \quad (18)$$

$$[\mathbf{P}_n^{(k)}]_{11} = \mathbf{a}_n^{(k)\dagger}\mathbf{a}_n^{(k)} - \sum_{l=1}^{k-1}|\mathbf{a}_n^{(l)\dagger}\mathbf{v}_n^{(k)} + \mathbf{v}_n^{(l)\dagger}\mathbf{a}_n^{(k)}|^2/d_{n,l}. \quad (19)$$

It turns out that $\mathbf{a}_n^{(k)}$ is a linear combination of the columns of $\mathbf{W}_n$ that can be expressed in a closed-form as shown in Lemma 3, which helps us to derive the statistics of $[\mathbf{C}_n^{(k)}]_{11}$ and $[\mathbf{P}_n^{(k)}]_{11}$ in Lemma 4.

Lemma 3: The $M_r \times 1$ vector $\mathbf{a}_n^{(k)}$ can be expressed as

$$\mathbf{a}_n^{(k)} = \mathbf{w}_n^{(k)} - \sum_{m=1}^{k-1}\varphi_{n,m}^{(k)}\mathbf{w}_n^{(k-m)}, \quad (20)$$

where $\mathbf{w}_n^{(k)}$ is the kth column of $\mathbf{W}_n$ and the linear combination coefficients can be computed iteratively using

$$\varphi_{n,m}^{(k)} = \frac{1}{\sqrt{d_{n,k-m}}}\left(r_{n,(k-m)k} - \sum_{u=1}^{m-1}\varphi_{n,u}^{(k)}r_{n,(k-m)(k-u)}\right), \quad \text{for } 1 \le m \le k-1. \quad (21)$$

Proof: See Appendix C.

Given the current bit loading we know from [33] that the optimal predictor that minimizes the mean squared prediction error $\mathrm{E}\left[\|\mathbf{b}_{n+1} - \widetilde{\mathbf{b}}_{n+1}\|^2\right]$ is the conditional mean $\widetilde{\mathbf{b}}_{n+1}^{opt} = \mathrm{E}\left[\mathbf{b}_{n+1}|\mathbf{b}_n\right]$. When the elements of $\mathbf{H}_n$ are i.i.d complex Gaussian variables with zero mean and unit variance, the two matrices $\mathbf{Q}_n$ and $\mathbf{R}_n$ in the QR decomposition of $\mathbf{H}_n$ are independent [34]. Moreover, the elements of $\mathbf{R}_n$, $\{r_{n,ij}\}_{1\le i\le j\le M_t}$, are independent. $\{r_{n,ij}\}_{i<j}$ are complex Gaussian random variables with zero mean and unit variance and $2r^2_{n,ii}$ is a Chi-squared random variable with degree of freedom $2(M_r-i+1)$ [34]. Using these properties, we can obtain $\mathrm{E}\left[\mathbf{b}_{n+1}|\mathbf{b}_n\right]$ from $\mathrm{E}\left[\mathbf{b}_{n+1}|\mathbf{H}_n\right]$ by averaging over $\mathbf{Q}_n$ and $\{r_{n,ij}, i<j\}$; that is

$$\widetilde{\mathbf{b}}_{n+1}^{opt} = \mathrm{E}_{\{r_{n,ij},i<j\}} \cdot \left[\mathrm{E}_{\{[\mathbf{Q}_n]_{ij},0\le i,j\le M_t\}}\left[\mathrm{E}\left[\mathbf{b}_{n+1}|\mathbf{H}_n = \mathbf{Q}_n\mathbf{R}_n\right]\right]\right], \quad (22)$$

where the notations $\mathrm{E}_{\{y_i\}}[\cdot]$ denotes expectation taken with respect to a set of random variables $\{y_i\}$. To derive the optimal $\widetilde{\mathbf{b}}_{n+1}^{opt}$, let us begin with the expectation $\mathrm{E}\left[\mathbf{b}_{n+1}|\mathbf{H}_n\right]$ first. When $\mathbf{H}_n$ is given, using the expression of $b_{n+1,k}$ in (17) we have

$$\mathrm{E}\left[b_{n+1,k}|\mathbf{H}_n\right] \approx b_{n,k} + \frac{\epsilon^2}{\log_e(2)} \cdot \left(\frac{\mathrm{E}\left[[\mathbf{P}_n^{(k)}]_{11}|\mathbf{H}_n\right] - d_{n,k}}{\gamma_k^{-1}+d_{n,k}} - \frac{\mathrm{E}\left[[\mathbf{C}_n^{(k)}]_{11}^2|\mathbf{H}_n\right]}{2(\gamma_k^{-1}+d_{n,k})^2}\right), \quad (23)$$

where we have used $\mathrm{E}\left[[\mathbf{C}_n^{(k)}]_{11}|\mathbf{H}_n\right] = 0$, a property coming from the fact that $\{\mathbf{w}_n^{(i)}\}_{i=1}^k$ are i.i.d. circularly symmetric complex Gaussian random vectors. From (23), We can see that $\mathrm{E}\left[b_{n+1,k}|\mathbf{H}_n\right]$ depends on the expectations of $[\mathbf{C}_n^{(k)}]_{11}^2|\mathbf{H}_n$ and $[\mathbf{P}_n^{(k)}]_{11}|\mathbf{H}_n$, to be given in Lemma 4.

Lemma 4: When the channel $\mathbf{H}_n$ is given, $[\mathbf{C}_n^{(k)}]_{11}$ has zero mean and its variance is given by

$$\mathrm{E}\left[[\mathbf{C}_n^{(k)}]_{11}^2|\mathbf{H}_n\right] = 2d_{n,k}\left(1+\sum_{m=1}^{k-1}|\varphi_{n,m}^{(k)}|^2\right). \quad (24)$$

The mean of $[\mathbf{P}_n^{(k)}]_{11}$ given $\mathbf{H}_n$ is

$$\mathrm{E}\left[[\mathbf{P}_n^{(k)}]_{11}|\mathbf{H}_n\right] = (M_r-k+1)\left(1+\sum_{m=1}^{k-1}|\varphi_{n,m}^{(k)}|^2\right) - \sum_{l=1}^{k-1}\frac{d_{n,k}}{d_{n,l}}\left(1+\sum_{m=1}^{l-1}|\varphi_{n,m}^{(l)}|^2\right). \quad (25)$$

Proof: See Appendix D.

Using Lemma 4 and (23), we can see that $\mathrm{E}\left[\mathbf{b}_{n+1}|\mathbf{H}_n\right]$ depends on $r_{n,ij}$ only, but not on $\mathbf{Q}_n$. As a result, the optimal predictor in (22) can be rewritten as

$$\widetilde{\mathbf{b}}_{n+1}^{opt} = \mathrm{E}_{r_{n,ij},i<j}\left[\mathrm{E}\left[\mathbf{b}_{n+1}|\mathbf{H}_n\right]\right]. \quad (26)$$

Combining the results in (23)–(26), we obtain the optimal predictor of bit loading in Theorem 1.

Theorem 1: When $\mathbf{b}_n$ is given, the optimal predictor of bit loading $b_{n+1,k}$ is given by

$$\widetilde{b}_{n+1,k}^{opt} \approx b_{n,k} + \frac{\epsilon^2}{\log_e(2)}\left(\frac{\Omega_n^{(k)}-d_{n,k}}{\gamma_k^{-1}+d_{n,k}} - \frac{\Psi_n^{(k)}}{2(\gamma_k^{-1}+d_{n,k})^2}\right), \quad (27)$$

where

$$\Psi_n^{(k)} = 2d_{n,k}\prod_{m=1}^{k-1}\left(1+\frac{1}{d_{n,m}}\right), \quad (28)$$

$$\Omega_n^{(k)} = (M_r-k+1)\prod_{m=1}^{k-1}\left(1+\frac{1}{d_{n,m}}\right) - \sum_{j=1}^{k-1}\frac{d_{n,k}}{d_{n,j}}\prod_{m=1}^{j-1}\left(1+\frac{1}{d_{n,m}}\right). \quad (29)$$

Proof: See Appendix E.

From Theorem 1, we can see that $\widetilde{b}_{n+1,k}^{opt}$ can be obtained from γ_k, $\Psi_n^{(k)}$ and $\Omega_n^{(k)}$. Both $\Psi_n^{(k)}$ and $\Omega_n^{(k)}$ can be computed once $\{d_{n,m}\}_{m=1}^k$ is known, which can be obtained from bit loading using $d_{n,m} = (2^{b_{n,m}} - 1)/\gamma_m$ as $b_{n,m} = \log_2(1 + \gamma_m d_{n,m})$. Since $\gamma_k = P_0/(\Gamma_k M_t N_0)$, the optimal predictor $\widetilde{b}_{n+1,k}^{opt}$ can be computed using the bit loading at time n and no extra side information is needed. In next section, we will derive the statistics of prediction error using the results in Theorem 1.

V. Quantization of Prediction Error

In the proposed predictive quantization system, the prediction error $\boldsymbol{\delta}_{n+1} = \mathbf{b}_{n+1} - \widetilde{\mathbf{b}}_{n+1}$ is quantized and sent back to the transmitter. It is known that, if the quantizer is designed according to the statistics of $\boldsymbol{\delta}_{n+1}$, a smaller quantization error can be achieved. Combining (17) and (27), we have

$$\delta_{n+1,k} \approx \frac{\epsilon}{\log_e(2)}\left(\frac{[\mathbf{C}_n^{(k)}]_{11}}{\gamma_k^{-1} + d_{n,k}}\right) + \frac{\epsilon^2}{\log_e(2)}\left(\frac{[\mathbf{P}_n^{(k)}]_{11} - \Omega_n^{(k)}}{\gamma_k^{-1} + d_{n,k}} - \frac{[\mathbf{C}_n^{(k)}]_{11}^2 - \Psi_n^{(k)}}{2(\gamma_k^{-1} + d_{n,k})^2}\right). \quad (30)$$

When the optimal predictor in (27) is used, we have $\mathrm{E}[\delta_{n+1,k}|\mathbf{b}_n] = 0$ as $\widetilde{\mathbf{b}}_{n+1}^{opt}$ is the mean of $\mathbf{b}_{n+1}$ conditioned on $\mathbf{b}_n$. Let $\sigma^2_{\delta_{n+1,k}|\mathbf{b}_n}$ be the variance of $\delta_{n+1,k}$ given the bit loading $\mathbf{b}_n$, i.e., $\sigma^2_{\delta_{n+1,k}|\mathbf{b}_n} = \mathrm{E}[(b_{n+1,k} - \widetilde{b}_{n+1,k})^2|\mathbf{b}_n]$. Using the approximation of $\delta_{n+1,k}$ in (30) and the results in Theorem 1, we can verify that $\sigma^2_{\delta_{n+1,k}|\mathbf{b}_n}$ has the following second order approximation,

$$\sigma^2_{\delta_{n+1,k}|\mathbf{b}_n} \approx 2d_{n,k}\prod_{m=1}^{k-1}\left(1 + \frac{1}{d_{n,m}}\right)\left[\frac{\epsilon}{\log_e(2)(\gamma_k^{-1} + d_{n,k})}\right]^2. \quad (31)$$

We can see that the conditional variance $\sigma^2_{\delta_{n+1,k}|\mathbf{b}_n}$ depends only on $\{d_{n,m}\}_{m=1}^k$. Therefore, $\sigma^2_{\delta_{n+1,k}|\mathbf{b}_n}$ can also be computed using the bit loading at time n like the optimal predictor. Now we can design the quantizer according to $\sigma^2_{\delta_{n+1,k}|\mathbf{b}_n}$.

A. Quantizer Design

For the quantization of prediction error $\delta_{n,k}$, a smaller quantization error can be achieved if the quantizer can be designed according to the distribution of $\delta_{n,k}$ [31]. From the expression in (30), we can see that the first term on the right-hand side, i.e., the dominating term, is a complex Gaussian random variable when $\mathbf{H}_n$ is given. We can see this by observing that the elements of $\mathbf{W}_n$ are Gaussian. Using (13) we can see that $[\mathbf{C}_n^{(k)}]_{11}$ is a linear combination of Gaussian random variables when $\mathbf{H}_n$ is given. Thus $[\mathbf{C}_n^{(k)}]_{11}$ is a complex Gaussian random variable when $\mathbf{H}_n$ is given. We will demonstrate through simulations that given $\mathbf{b}_n$, the distribution of $\delta_{n+1,k}$ is well approximated by a complex Gaussian random variable and the approximation of variance given in (31) is a very good one. The optimal quantizer for a Gaussian source can be found in, e.g., [31]. Given a zero mean complex Gaussian random variable with variance $\sigma^2_{\delta_{n+1,k}|\mathbf{b}_n}$, the optimal reproduction points can be obtained in terms of the variance [31]. Since $\sigma^2_{\delta_{n+1,k}|\mathbf{b}_n}$ is a function of bit loading vector $\mathbf{b}_n$, the reproduction points can be adapted with time. In the following, we summarize the algorithm of predictive feedback of bit loading with adaptive quantization.

Algorithm of the Proposed PQB: The predictor given in Theorem 1 and the above quantizer design are derived based on the unquantized bit loading. However, at time $n+1$ the transmitter knows only the quantized $\widehat{b}_{n,k}$, but not $b_{n,k}$. When the prediction error is small, $\widehat{b}_{n,k} \approx b_{n,k}$, the predictor in Theorem 1 can be approximated by replacing the unquantized bit loading with the quantized $\widehat{b}_{n,k}$. Initially, set the bit loading at time $n = 0$ to be $b_{ini,k} = \log_2(1+\gamma_k \mathrm{E}[r_{n,kk}^2])$ for $k = 1, 2, \ldots, M_t$, which is the upper bound of the averaged bit loading[1]. Let the quantized bit loading at time n be $\widehat{\mathbf{b}}_n$. At time $n+1$, the following steps are performed.

1) Both the transmitter and receiver compute the optimal predictor $\widetilde{\mathbf{b}}_{n+1}$ in (27) and the variance $\sigma^2_{\delta_{n+1,k}|\mathbf{b}_n}$ in (31) using the quantized bit loading $\widehat{\mathbf{b}}_n$[2].
2) At the receiver, quantize $\delta_{n+1,k}$ to $\widehat{\delta}_{n+1,k}$ using a quantizer that is adapted according to $\sigma^2_{\delta_{n+1,k}|\mathbf{b}_n}$. The quantized prediction error $\widehat{\delta}_{n+1,k}$ is fed back to the transmitter.
3) At the transmitter, the quantized bit loading at time $n+1$ is obtained by $\widehat{\mathbf{b}}_{n+1} = \widehat{\boldsymbol{\delta}}_{n+1} + \widetilde{\mathbf{b}}_{n+1}$.

In the above derivations of bit loading, we assume reverse detection ordering is used for the decision feedback receiver. After bit loading is quantized, the receiver can still choose a detection ordering that is optimal in certain sense, e.g., the optimal ordering for minimizing the worst subchannel symbol error rate. For uniform bit loading, the optimal ordering that minimizing the worst subchannel error rate is given by the VBLAST receiver [36]. When the bit loading is not uniform, the optimal solution is the ordering based on the rate-normalized-SNR [37], which is the subchannel SNR normalized by a rate-related term, i.e., $P_0/\left(M_t\sigma^2_{e_{n,k}}(2^{\lfloor\widehat{b}_{n,k}\rfloor} - 1)\right)$ [38]. In a VBLAST receiver, detection is done iteratively and in each iteration the subchannel that has the largest SNR is decoded. When the detection ordering is based on rate-normalized SNR, the detection is also done in an iterative manner like VBLAST, but the subchannel with the largest rate-normalized SNR is decoded, instead of the subchannel with the largest SNR.

1) Feedback Rate B: For the proposed PQB method, feedback rate B means that the number of total bits used for quantization for each feedback is B. For example, suppose $B = 4$ and 2 bits or 4 bits quantizer is used to quantize the prediction error $\delta_{n+1,k}$. If the number of used subchannels is 1, 4 bits quantizer is used to quantize $\delta_{n+1,0}$. If the number of used subchannels is great than 1, 2 bits quantizer is used to quantize $\delta_{n+1,k}$ and for each feedback time only the bit loadings of two subchannels are fed back to the transmitter.

[1]At the initial time $n = 0$, the transmitter does not have any information of the transmission rate for the variable rate system. One way to determine the initial bit loading is to use the statistics of $r_{n,ii}$. Using Jensen's inequality, it can be shown that $\mathrm{E}[b_{n,k}] \leq b_{ini,k}$, where $b_{ini,k} = \log_2(1 + \gamma_k \mathrm{E}[r_{n,kk}^2])$. The expectation $\mathrm{E}[r_{n,kk}^2]$ can be obtained in a closed form as $\mathrm{E}[r_{n,kk}^2] = M_r - k + 1$.

[2]The optimal predictor $\widetilde{\mathbf{b}}_{n+1}$ in (27) and the variance $\sigma^2_{\delta_{n+1,k}|\mathbf{b}_n}$ in (31) are derived when the loading at time n is given. However, the transmitter only has the quantized version of bit loading at time n. When the quantization error is small, we have $\widehat{\mathbf{b}}_n \to \mathbf{b}_n$. Thus in the proposed PQB algorithm we assume the quantization error is small and use $\widehat{\mathbf{b}}_n$ to compute the predictor of bit loading at time $n+1$.

TABLE I
SIMULATION ENVIRONMENT PARAMETERS

	micro-cellular	urban
carrier frequency (GHz)	2.5	2.0
terminal speed (km/h)	3	30

2) The Case $M_r < M_t$ and Variable Number of Subchannels: In the above derivation, we have assumed that $M_r \geq M_t$ and the number of subchannels used for transmission is M_t. Each subchannel is assigned power P_0/M_t even if the number of bits loaded is less than one. Now we consider the more general case that the condition $M_r \geq M_t$ is removed. To achieve a higher transmission rate, we allow the number of subchannels used for transmission M to vary between 1 and $\min(M_r, M_t)$ and each subchannel is given power P_0/M similar to [26]. In this case, there are $M_t - M$ subchannels that are not assigned any bits. Let $\mathbf{b}'_n$ be the reduced bit loading vector that is obtained by removing the zero entries of $\mathbf{b}_n$. Let $\mathbf{H}'_n$ be the $M_r \times M$ reduced channel matrix that is obtained by removing the $M_t - M$ columns of $\mathbf{H}_n$ that correspond to the zero entries of $\mathbf{b}_n$. Then we can apply the proposed PQB algorithm on $\mathbf{b}'_n$. All the results in Lemma 1–4 and Theorem 1 continue to hold when we replace $\mathbf{b}_n$ and $\mathbf{H}_n$ respectively by $\mathbf{b}'_n$ and $\mathbf{H}'_n$. The optimal value of M and the corresponding subset of used subchannels can be chosen to maximize the transmission rate. To inform the transmitter of the change of used subchannels, we can feed back the information of the optimal subset, say, every S channel uses, which is called refresh period in simulations.

Remarks: In [26], predictive coding was also used for quantizing bit loading, but there are some important differences. The receiver in [26] is linear rather than a decision feedback receiver. The optimal predictor in (27) is obtained using the Cholesky decomposition of the channel Gram matrix, and the prediction error is approximated in a closed form. In [26], only the upper and lower bounds of the optimal predictor and prediction error are given, but explicit formulations are not available.

VI. SIMULATIONS

In this section, we use Monte Carlo simulations to demonstrate the performance of the proposed PQB feedback system. In the proposed PQB algorithm, $\widehat{\delta}_{n+1,k}$ is sent back to the transmitter using a feedback channel with feedback rate B, which is the number of bits sent back to the transmitter per channel use. Three transmission scenarios, indoor, micor-cellular and urban [35], are considered as listed in Table I. In examples 1–2, the time varying MIMO channel $\mathbf{H}_n$ is generated using the Gauss-Markov model in (1). The values of ϵ corresponding to these three scenarios are respectively 0.06 and 0.47. We consider the case $M_r = 4$ and $M_t = 2$. The total transmit power to noise ratio P_0/N_0 is 12 dB. The number of subchannels used for transmission is 2, and $\xi_k = \xi = 10^{-3}$. In examples 3–4, the channel is generated using the filtering method [39] for the same Doppler frequency in the micro-cellular and urban scenarios. $M_r = 6$ and $M_t = 4$, and the number of subchannels used is updated periodically with period 100. To avoid extra feedback, the first few feedback bits of each refresh period is used to inform the transmitter of the used subchannels. The transmission rate at the end of a period is used to initialize the bit loading of the next period by uniformly distributing the transmission bits to the used subchannels.

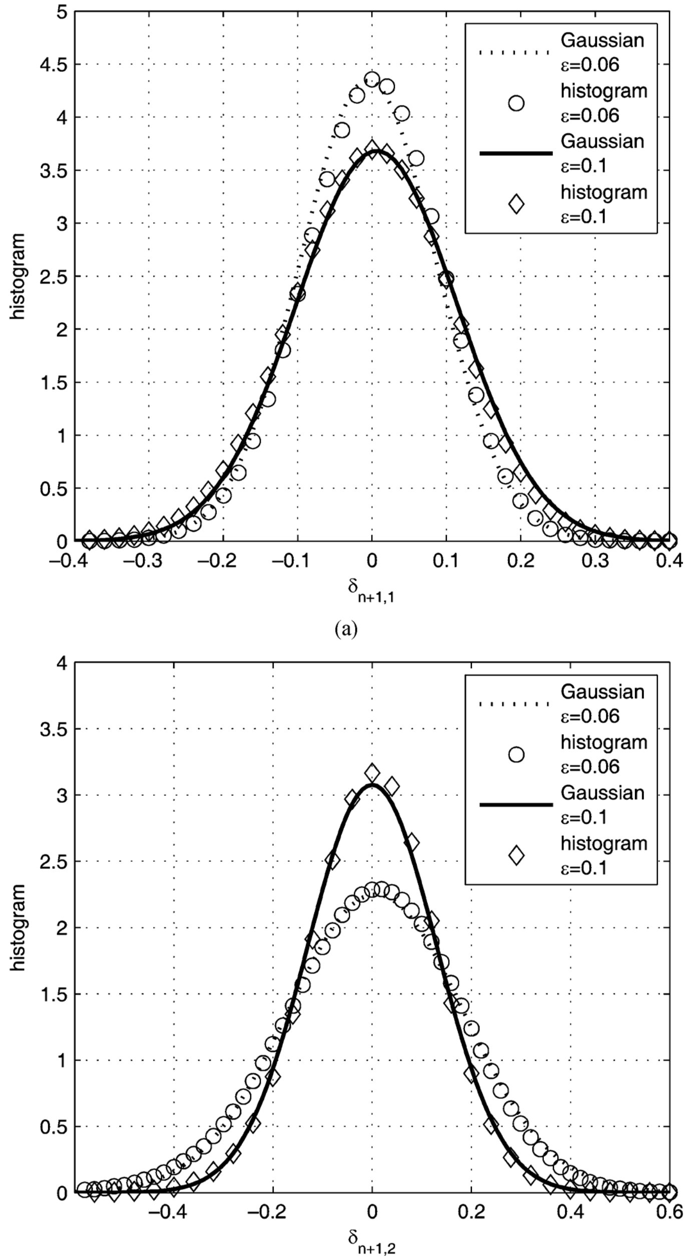

Fig. 2. The histograms of subchannel prediction error $\delta_{n+1,k}$ and Gaussian pdf with zero mean and variance computed from (31); (a) $k = 1$ and (b) $k = 2$.

1) Example 1. Histogram of Prediction Error: Fig. 2 show the histogram of $\delta_{n+1,k}$ for $\epsilon = 0.06$ and 0.1 when the previous bit loading $\mathbf{b}_n$ is given. The case $\epsilon = 0.1$ corresponds to the indoor scenario with terminal speed 4 km/h. Given a bit loading vector, or equivalently $\{r_{n,ii}\}_{i=1}^{M_t}$, the histogram is generated using 10^4 random realizations of $\{r_{n,ij}\}_{i<j}$, $\mathbf{Q}_n$, and $\mathbf{W}_n$. For each ϵ, we also show the pdf of a zero mean Gaussian random variable with variance computed using (31). We can see that the prediction errors are well approximated by Gaussian random variables and the approximation in (31) is a good one.

2) Example 2. Quantization Error Versus Feedback Rate: Fig. 3 shows the mean squared quantization error (MSE), i.e.,

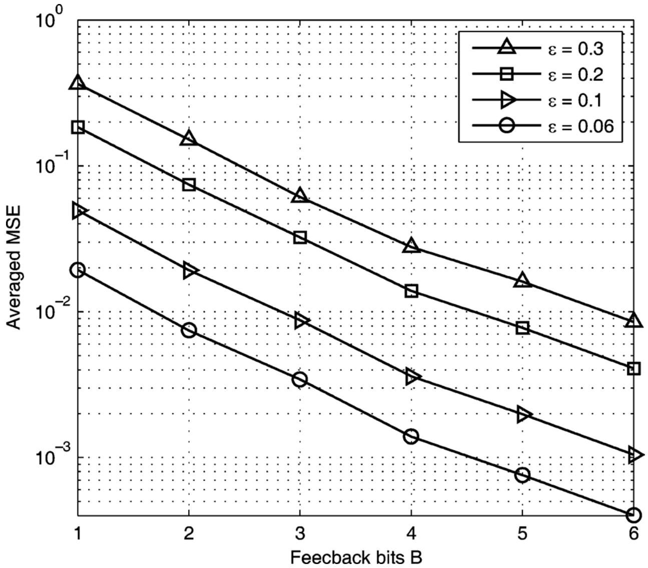

Fig. 3. Mean squared quantization error as a function of feedback rate B.

$\mathrm{E}\left[\sum_{k=1}^{M_t} |b_{n,k} - \widehat{b}_{n,k}|^2\right]$, as a function of the feedback rate B for different ϵ. In Fig. 3, four values of ϵ are considered. The case $\epsilon = 0.06$ are taken from Table I, $\epsilon = 0.1$ corresponds to the indoor scenario with terminal speed 4 km/h, while $\epsilon = 0.2$ and 0.3 correspond to the Urban scenario when the terminal speeds are 12.5 km/h and 18.5 km/h, respectively. The MSEs in Fig. 3 are obtained by averaging over 10^6 channel realizations. From Fig. 3, we can see that the MSE is proportional to ϵ^2 for a given feedback rate. For example, when $B = 6$, MSE is respectively 0.001 and 0.0041 for $\epsilon = 0.1$ and 0.2. When ϵ increases from 0.1 to 0.2, MSE increases by approximately 4 times. The reason is as follows. We know the quantization error $\mathbf{b}_{n+1} - \widehat{\mathbf{b}}_{n+1}$ is exactly the same as the quantization error $\boldsymbol{\delta}_{n+1} - \widehat{\boldsymbol{\delta}}_{n+1}$. Also the variance of quantization error is proportional to the variance of the signal to be quantized [31]. As the variance of the prediction error is proportional to ϵ^2 in (31), we see that MSE is proportional to ϵ^2 for a given feedback rate.

3) Example 3. Bit Error Rate Performance: Fig. 4(a) and (b) show the bit error rate performance of PQB respectively for (a) micro-cellular and (b) urban scenarios. To have an integer bit loading, we truncate $b_{n,k}$ to the nearest integer and the transmission rate is $\sum_{k=1}^{M} \lfloor b_{n,k} \rfloor$. For comparison, we also show the performance of per-antenna-rate-control (PARC) system in [16] and precoder systems in [20] and [23], in which the precoder is updated based on the feedback information. For PARC, the power is equally divided among the subchannels that are used for transmission and the quantized integer bit loading $\lfloor b_{n,k} \rfloor$ is directly fed back to the transmitter. For example, suppose two subchannels are used for transmission. Then each of the two subchannels used are allocated with power $P_0/2$. The subset of subchannels used for transmission is chosen using the capacity maximizing criterion. The receiver chooses the subset that would result in the largest capacity. It is shown in [16] that with this suboptimal power allocation, the capacity loss (compared to the case of optimal power allocation) is almost negligible, but the complexity is lower. In [20], the channel Gram matrix is fed back based on geodesic curves (labeled as "geodesic curves"), and in [23]

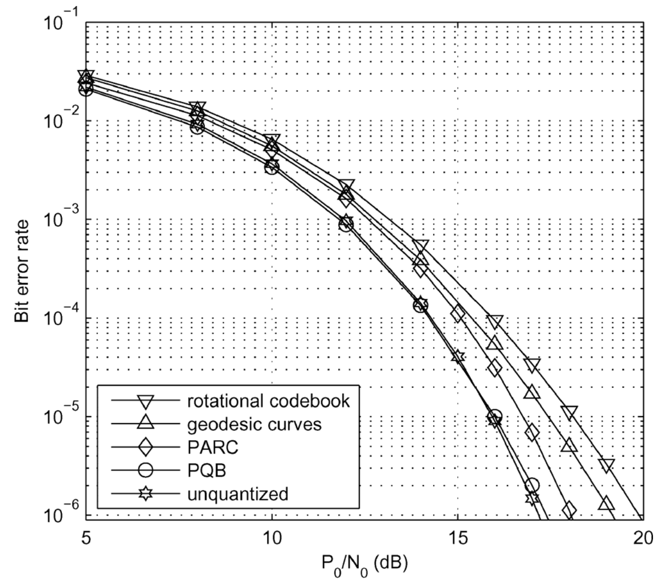

(a)

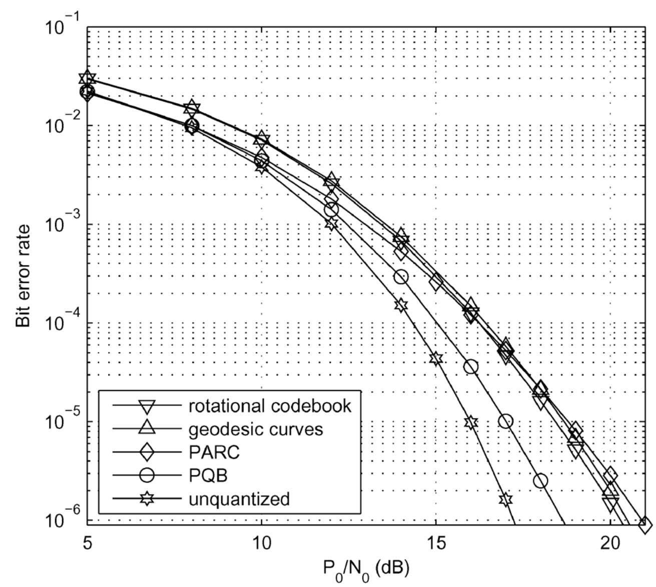

(b)

Fig. 4. Average bit error rate performance as a function of P_0/N_0 for $B = 2$; (a) micro-cellular scenario and (b) urban scenario.

the precoder is fed back using the rotation based differential precoder codebook (labeled as "rotational codebook"). For each data point in the plots, the average transmission rate of PQB and PARC is 12 bits or slightly over 12 bits per channel use. This is done by choosing an appropriate SNR gap Γ for a given P_0/N_0. For both [20] and [23], three substreams are transmitted and we use uniform bit loading (each subchannel loaded with 4 bits). The bit error rate is obtained by averaging over 10^7 channel realizations. For all the feedback schemes, feedback rate $B = 2$ is used. For the micro-cellular scenario in Fig. 4(a), the performance of PQB is very close to that of the "unquantized", for which the unquantized bit loading is assumed to be available to the transmitter. From Fig. 4(b), we can see that PQB system is around 2 dB better than the others when the bit error rate is 10^{-6}. Although the proposed PQB

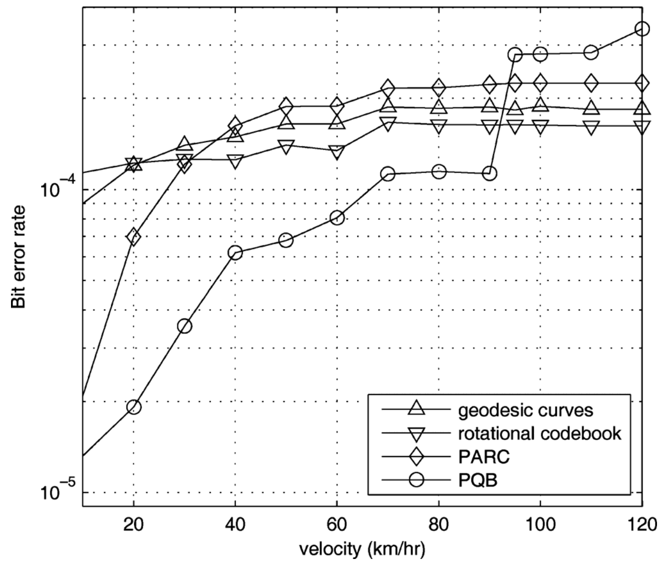

Fig. 5. Bit error rate as a function of terminal speed.

system is designed for a slowly time-varying channel, it can still achieve a very good performance in the urban scenario.

4) Example 4. Performance as a Function of Terminal Speed: Fig. 5 shows the bit error rate performance as a function of terminal speed for the 4 feedback schemes in Example 3. The carrier frequency is 2 GHz. $P_0/N_0 = 16$ dB and $B = 2$. For each data point in the plots, the average transmission rate of PQB and PARC is 12 bits or slightly over 12 bits per channel use. The bit error rate is obtained by averaging over 10^7 channel realizations. PARC and PQB are similar when terminal speed is low and the channel is almost time invariant. As speeds increases, the gap between the two widens. Fig. 5 shows that PQB is better when the terminal speed is less than 90 Km/hr. When the terminal speed increases further, the there is little correlation between channels of consecutive time. In this case, the proposed PQB cannot take advantage from the temporal correlation of channel and it is better to switch to non differential feedback schemes.

VII. Conclusion

In this paper, we consider a variable-rate MIMO system with a decision feedback receiver. The bit loading is dynamically assigned to the subchannels as per antenna rate control so that the transmission rate is adapted according to the current channel condition. Predictive quantization, which is known to be very useful for coding correlated signals, is used to quantize the bit loading for feedback. When reverse detection ordering is used at the receiver, the bit loading is related to the Cholesky decomposition of the channel Gram matrix. By modeling the channel as a first-order Gauss-Markov process, we show that the nested submatrices in the Cholesky decomposition can be updated as time evolves. Using the update, we derive the optimal predictor of the next bit loading in a closed-form. The statistics of the prediction error have also been derived and exploited in the design of the quantizer to achieve a smaller quantization error. Although the derivations are carried out for a small ϵ, simulations demonstrate that PQB gives a good tracking performance even when the channel does not change slowly.

Appendix A
Proof of Lemma 1

We will prove (10) by the mathematical induction. For $k = 1$, $\mathbf{T}_n^{(1)} = \mathbf{H}_n^\dagger \mathbf{H}_n = \mathbf{H}_n^{(1)\dagger}\mathbf{H}_n^{(1)}$. Suppose (10) holds for $k = k_0$. Decompose $\mathbf{T}_n^{(k_0)}$ as

$$\mathbf{T}_n^{(k_0)} = \begin{bmatrix} 1 & \mathbf{0} \\ \tilde{\boldsymbol{\ell}}_n^{(k_0)} & \mathbf{I}_{M_t-k_0} \end{bmatrix} \begin{bmatrix} d_{n,k_0} & \mathbf{0} \\ \mathbf{0} & \mathbf{T}_n^{(k_0+1)} \end{bmatrix} \begin{bmatrix} 1 & \tilde{\boldsymbol{\ell}}_n^{(k_0)\dagger} \\ \mathbf{0} & \mathbf{I}_{M_t-k_0} \end{bmatrix}. \tag{32}$$

Let $\mathbf{U}_n^{(k_0)} = \begin{bmatrix} 1 & \tilde{\boldsymbol{\ell}}_n^{(k_0)\dagger} \\ \mathbf{0} & \mathbf{I}_{M_t-k_0} \end{bmatrix}$. Then $\left(\mathbf{U}_n^{(k_0)}\right)^{-1} = \begin{bmatrix} 1 & -\tilde{\boldsymbol{\ell}}_n^{(k_0)\dagger} \\ \mathbf{0} & \mathbf{I}_{M_t-k_0} \end{bmatrix}$. Let $\mathbf{v}_n^{(k_0)}$ be the first column of $\mathbf{H}_n^{(k_0)}$. Using $\mathbf{T}_n^{(k_0)} = \mathbf{H}_n^{(k_0)\dagger}\mathbf{H}_n^{(k_0)}$ and multiplying the left-hand side and right-hand side of (32) by $\left(\mathbf{U}_n^{(k_0)\dagger}\right)^{-1}$ and $\left(\mathbf{U}_n^{(k_0)}\right)^{-1}$, respectively, we have

$$\begin{aligned} &\left(\mathbf{U}_n^{(k_0)\dagger}\right)^{-1}\mathbf{T}_n^{(k_0)}\left(\mathbf{U}_n^{(k_0)}\right)^{-1} \\ &= \left[\mathbf{v}_n^{(k_0)} \quad \mathbf{H}_n^{(k_0)}\begin{bmatrix} -\tilde{\boldsymbol{\ell}}_n^{(k_0)\dagger} \\ \mathbf{I}_{M_t-k_0}\end{bmatrix}\right]^\dagger \left[\mathbf{v}_n^{(k_0)} \quad \mathbf{H}_n^{(k_0)}\begin{bmatrix} -\tilde{\boldsymbol{\ell}}_n^{(k_0)\dagger} \\ \mathbf{I}_{M_t-k_0}\end{bmatrix}\right] \end{aligned} \tag{33}$$

$$= \left[\mathbf{v}_n^{(k_0)} \quad \mathbf{H}_n^{(k_0+1)}\right]^\dagger \left[\mathbf{v}_n^{(k_0)} \quad \mathbf{H}_n^{(k_0+1)}\right] \tag{34}$$

$$= \begin{bmatrix} d_{n,k_0} & \mathbf{0} \\ \mathbf{0} & \mathbf{T}_n^{(k_0+1)} \end{bmatrix}, \tag{35}$$

where $\mathbf{v}_n^{(k_0)}$ is the first column of $\mathbf{H}_n^{(k_0)}$. Comparing (34) and (35), we have $\mathbf{T}_n^{(k_0+1)} = \mathbf{H}_n^{(k_0+1)\dagger}\mathbf{H}_n^{(k_0+1)}$. So (10) holds for $k = k_0 + 1$ as well and the proof of (10) is complete. Since (10) is true, the (34) and (35) hold for $1 \le k_0 \le M_t - 1$. Thus we can conclude that $\mathbf{v}_n^{(k_0)\dagger}\mathbf{H}_n^{(k_0+1)} = \mathbf{0}$ for $1 \le k_0 \le M_t - 1$, which means that the first column of $\mathbf{H}_n^{(k_0)}$ is orthogonal to each column of $\mathbf{H}_n^{(k_0+1)}$. $\triangle\triangle\triangle$

Appendix B
Proof of Lemma 2

We prove Lemma 2 by induction. We know $\mathbf{T}_{n+1}^{(1)} = \mathbf{H}_{n+1}\dagger\mathbf{H}_{n+1}$. Using the Gauss-Markov model in (1) and the approximation $\epsilon\sqrt{1-\epsilon^2} \approx \epsilon$, we have

$$\mathbf{T}_{n+1}^{(1)} \approx \mathbf{T}_n^{(1)} + \epsilon\mathbf{C}_n^{(1)} + \epsilon^2(\mathbf{P}_n^{(1)} - \mathbf{T}_n^{(1)}), \tag{36}$$

where $\mathbf{C}_n^{(1)} = \mathbf{H}_n^\dagger\mathbf{W}_n + \mathbf{W}_n^\dagger\mathbf{H}_n$, $\mathbf{P}_n^{(1)} = \mathbf{W}_n^\dagger\mathbf{W}_n$. Suppose Lemma 2 holds for $k = k_0$. Then we have

$$\mathbf{T}_{n+1}^{(k_0)} \approx \mathbf{T}_n^{(k_0)} + \epsilon\mathbf{C}_n^{(k_0)} + \epsilon^2(\mathbf{P}_n^{(k_0)} - \mathbf{T}_n^{(k_0)}), \tag{37}$$

where the $(M_t - k_0 + 1) \times (M_t - k_0 + 1)$ matrix $\mathbf{C}_n^{(k_0)}$ is given by

$$\mathbf{C}_n^{(k_0)} = \mathbf{H}_n^{(k_0)\dagger}\mathbf{W}_n^{(k_0)} + \mathbf{W}_n^{(k_0)\dagger}\mathbf{H}_n^{(k_0)}, \tag{38}$$

and the $(M_t - k_0 + 1) \times (M_t - k_0 + 1)$ matrix $\mathbf{P}_n^{(k_0)}$ is given by

$$\begin{aligned} \mathbf{P}_n^{(k_0)} = \mathbf{W}_n^{(k_0)\dagger}\mathbf{W}_n^{(k_0)} - \sum_{m=1}^{k_0-1}(1/d_{n,m})(\mathbf{a}_n^{(m)\dagger}\mathbf{H}_n^{(k_0)} \\ + \mathbf{v}_n^{(m)\dagger}\mathbf{W}_n^{(k_0)})^\dagger(\mathbf{a}_n^{(m)\dagger}\mathbf{H}_n^{(k_0)} + \mathbf{v}_n^{(m)\dagger}\mathbf{W}_n^{(k_0)}). \end{aligned} \tag{39}$$

Now consider the case when $k = k_0+1$. Let us partition $\mathbf{W}_n^{(k_0)}$ and $\mathbf{H}_n^{(k_0)}$ as

$$\mathbf{W}_n^{(k_0)} = [\,\mathbf{a}_n^{(k_0)} \quad \mathbf{A}_n^{(k_0)}\,], \;\; \mathbf{H}_n^{(k_0)} = [\,\mathbf{v}_n^{(k_0)} \quad \mathbf{V}_n^{(k_0)}\,], \quad (40)$$

where $\mathbf{a}_n^{(k_0)}$ and $\mathbf{v}_n^{(k_0)}$ are $M_r \times 1$ vectors. $\mathbf{A}_n^{(k_0)}$ and $\mathbf{V}_n^{(k_0)}$ are $M_r \times (M_t - k_0)$ matrices. Using (37)–(40) and partitioning $\mathbf{T}_{n+1}^{(k_0)}$ as in (7), we obtain d_{n+1,k_0}, $\boldsymbol{\ell}_{n+1}^{(k_0)}$, and $\boldsymbol{\Phi}_{n+1}^{(k_0)}$, respectively, as

$$\begin{aligned} &d_{n+1,k_0} \\ &= d_{n,k_0} + \epsilon(\mathbf{v}_n^{(k_0)\dagger}\mathbf{a}_n^{(k_0)} + \mathbf{a}_n^{(k_0)\dagger}\mathbf{v}_n^{(k_0)}) \\ &\quad + \epsilon^2\Bigg[\mathbf{a}_n^{(k_0)\dagger}\mathbf{a}_n^{(k_0)} - \sum_{m=1}^{k_0-1}(1/d_{n,m})(\mathbf{a}_n^{(m)\dagger}\mathbf{v}_n^{(k_0)} \\ &\quad + \mathbf{v}_n^{(m)\dagger}\mathbf{a}_n^{(k_0)})^\dagger(\mathbf{a}_n^{(m)\dagger}\mathbf{v}_n^{(k_0)} + \mathbf{v}_n^{(m)\dagger}\mathbf{a}_n^{(k_0)}) - d_{n,k_0}\Bigg], \quad (41) \end{aligned}$$

$$\begin{aligned} &\boldsymbol{\ell}_{n+1}^{(k_0)} \\ &= \boldsymbol{\ell}_n^{(k_0)} + \epsilon(\mathbf{V}_n^{(k_0)\dagger}\mathbf{a}_n^{(k_0)} + \mathbf{A}_n^{(k_0)\dagger}\mathbf{v}_n^{(k_0)}) \\ &\quad + \epsilon^2\Bigg[\mathbf{A}_n^{(k_0)\dagger}\mathbf{a}_n^{(k_0)} - \sum_{m=1}^{k_0-1}(1/d_{n,m})(\mathbf{a}_n^{(m)\dagger}\mathbf{V}_n^{(k_0)} \\ &\quad + \mathbf{v}_n^{(m)\dagger}\mathbf{A}_n^{(k_0)})^\dagger(\mathbf{a}_n^{(m)\dagger}\mathbf{v}_n^{(k_0)} + \mathbf{v}_n^{(m)\dagger}\mathbf{a}_n^{(k_0)}) - \boldsymbol{\ell}_n^{(k_0)}\Bigg], \quad (42) \end{aligned}$$

$$\begin{aligned} &\boldsymbol{\Phi}_{n+1}^{(k_0)} \\ &= \boldsymbol{\Phi}_n^{(k_0)} + \epsilon(\mathbf{V}_n^{(k_0)\dagger}\mathbf{A}_n^{(k_0)} + \mathbf{A}_n^{(k_0)\dagger}\mathbf{V}_n^{(k_0)}) \\ &\quad + \epsilon^2\Bigg[\mathbf{A}_n^{(k_0)\dagger}\mathbf{A}_n^{(k_0)} - \sum_{m=1}^{k_0-1}(1/d_{n,m})(\mathbf{a}_n^{(m)\dagger}\mathbf{V}_n^{(k_0)} \\ &\quad + \mathbf{v}_n^{(m)\dagger}\mathbf{A}_n^{(k_0)})^\dagger(\mathbf{a}_n^{(m)\dagger}\mathbf{V}_n^{(k_0)} + \mathbf{v}_n^{(m)\dagger}\mathbf{A}_n^{(k_0)}) - \boldsymbol{\Phi}_n^{(k_0)}\Bigg]. \end{aligned} \quad (43)$$

Substituting (41)–(43) into (8) and approximating $\boldsymbol{\ell}_{n+1}^{(k_0)}\boldsymbol{\ell}_{n+1}^{(k_0)\dagger}/d_{n+1,k_0}$ using the second-order Taylor approximation, $\mathbf{T}_{n+1}^{(k_0+1)}$ can be expressed as

$$\mathbf{T}_{n+1}^{(k_0+1)} \approx \mathbf{T}_n^{(k_0+1)} + \epsilon\mathbf{C}_n^{(k_0+1)} + \epsilon^2(\mathbf{P}_n^{(k_0+1)} - \mathbf{T}_n^{(k_0+1)}), \quad (44)$$

where the $(M_t - k_0) \times (M_t - k_0)$ matrix $\mathbf{C}_n^{(k_0+1)}$ is given by

$$\begin{aligned} \mathbf{C}_n^{(k_0+1)} &= [\mathbf{V}_n^{(k_0)} - \mathbf{v}_n^{(k_0)}\tilde{\boldsymbol{\ell}}_n^{(k_0)\dagger}]^\dagger[\mathbf{A}_n^{(k_0)} - \mathbf{a}_n^{(k_0)}\tilde{\boldsymbol{\ell}}_n^{(k_0)\dagger}] \\ &\quad + [\mathbf{A}_n^{(k_0)} - \mathbf{a}_n^{(k_0)}\tilde{\boldsymbol{\ell}}_n^{(k_0)\dagger}]^\dagger[\mathbf{V}_n^{(k_0)} - \mathbf{v}_n^{(k_0)}\tilde{\boldsymbol{\ell}}_n^{(k_0)\dagger}] \\ &= \mathbf{H}_n^{(k_0+1)\dagger}\mathbf{W}_n^{(k_0+1)} + \mathbf{W}_n^{(k_0+1)\dagger}\mathbf{H}_n^{(k_0+1)}. \end{aligned} \quad (45)$$

In the second equality we have used $\mathbf{W}_n^{(k_0+1)} = \mathbf{W}_n^{(k_0)}\begin{bmatrix}-\tilde{\boldsymbol{\ell}}_n^{(k_0)\dagger} \\ \mathbf{I}_{M_t-k_0}\end{bmatrix} = \mathbf{A}_n^{(k_0)} - \mathbf{a}_n^{(k_0)}\tilde{\boldsymbol{\ell}}_n^{(k_0)\dagger}$ and $\mathbf{H}_n^{(k_0+1)} = \mathbf{H}_n^{(k_0)}\begin{bmatrix}-\tilde{\boldsymbol{\ell}}_n^{(k_0)\dagger} \\ \mathbf{I}_{M_t-k_0}\end{bmatrix} = \mathbf{V}_n^{(k_0)} - \mathbf{v}_n^{(k_0)}\tilde{\boldsymbol{\ell}}_n^{(k_0)\dagger}$. Similarly, the $(M_t - k_0) \times (M_t - k_0)$ matrix $\mathbf{P}_n^{(k_0+1)}$ is given by

$$\begin{aligned} \mathbf{P}_n^{(k_0+1)} &= \mathbf{W}_n^{(k_0+1)\dagger}\mathbf{W}_n^{(k_0+1)} \\ &\quad - \sum_{m=1}^{k_0}(1/d_{n,m})(\mathbf{a}_n^{(m)\dagger}\mathbf{H}_n^{(k_0+1)} + \mathbf{v}_n^{(m)\dagger}\mathbf{W}_n^{(k_0+1)})^\dagger \\ &\quad (\mathbf{a}_n^{(m)\dagger}\mathbf{H}_n^{(k_0+1)} + \mathbf{v}_n^{(m)\dagger}\mathbf{W}_n^{(k_0+1)}). \end{aligned} \quad (46)$$

Hence (12) holds for $k = k_0 + 1$. As $d_{n+1,k}$ is the top left element of $\mathbf{T}_{n+1}^{(k)}$, using (12) we can obtain the approximation in (15) and the proof is complete. △△△

Appendix C
Proof of Lemma 3

Let $\mathbf{u}_i^{(k)}$ be an $(M_t - k + 1) \times 1$ standard vector, i.e., $[\mathbf{u}_i^{(k)}]_i = 1$ and $[\mathbf{u}_i^{(k)}]_m = 0$ for $m \neq i$. Using the results in Lemma 2, the ith column of $\mathbf{W}_n^{(k+1)}$ is given by

$$\begin{aligned} &\mathbf{W}_n^{(k)}\mathbf{u}_i^{(k)} \\ &= \mathbf{W}_n^{(k-1)}\begin{bmatrix}-\tilde{\boldsymbol{\ell}}_n^{(k-1)\dagger} \\ \mathbf{I}_{M_t-k+1}\end{bmatrix}\mathbf{u}_i^{(k)} \\ &= \mathbf{W}_n^{(k-1)}\left(\begin{bmatrix}\mathbf{0}_{1\times(M-k+1)} \\ \mathbf{I}_{M_t-k+1}\end{bmatrix} + \begin{bmatrix}-\tilde{\boldsymbol{\ell}}_n^{(k-1)\dagger} \\ \mathbf{0}_{(M_t-k+1)\times(M_t-k+1)}\end{bmatrix}\right)\mathbf{u}_i^{(k)} \\ &= \mathbf{W}_n^{(k-1)}\mathbf{u}_{i+1}^{(k-1)} - \mathbf{a}_n^{(k-1)}[\tilde{\boldsymbol{\ell}}_n^{(k-1)*}]_i. \end{aligned} \quad (47)$$

Since $\mathbf{H}_n^\dagger\mathbf{H}_n = \mathbf{R}_n^\dagger\mathbf{R}_n = \mathbf{L}_n\mathbf{D}_n\mathbf{L}_n^\dagger$, we have $[\tilde{\boldsymbol{\ell}}_n^{(m)*}]_{s-m} = r_{n,ms}/\sqrt{d_{n,m}}$ for $m < s$. Using (47), $\mathbf{a}_n^{(k)} = \mathbf{W}_n^{(k)}\mathbf{u}_1^{(k)}$ can be expressed as

$$\begin{aligned} \mathbf{a}_n^{(k)} &= \mathbf{W}_n^{(k-1)}\mathbf{u}_2^{(k-1)} - \frac{r_{n,(k-1)k}}{\sqrt{d_{n,k-1}}}\mathbf{a}_n^{(k-1)} \\ &= \mathbf{W}_n^{(k-2)}\mathbf{u}_3^{(k-2)} - \frac{r_{n,(k-2)k}}{\sqrt{d_{n,k-2}}}\mathbf{a}_n^{(k-2)} - \frac{r_{n,(k-1)k}}{\sqrt{d_{n,k-1}}}\mathbf{a}_n^{(k-1)} \\ &= \mathbf{W}_n^{(1)}\mathbf{u}_k^{(1)} - \sum_{m=1}^{k-1}\frac{r_{n,mk}}{\sqrt{d_{n,m}}}\mathbf{a}_n^{(m)} \\ &= \mathbf{w}_n^{(k)} - \sum_{m=1}^{k-1}\frac{r_{n,mk}}{\sqrt{d_{n,m}}}\mathbf{a}_n^{(m)}, \end{aligned} \quad (48)$$

where $\mathbf{w}_n^{(k)}$ is the kth column of $\mathbf{W}_n$. Let $\varphi_{n,1}^{(k)} = r_{n,(k-1)k}/\sqrt{d_{n,k-1}}$. The vector $\mathbf{a}_n^{(k)}$ in (48) can be rewritten as

$$\mathbf{a}_n^{(k)} = \mathbf{w}_n^{(k)} - \varphi_{n,1}^{(k)}\mathbf{a}_n^{(k-1)} - \sum_{m=1}^{k-2}\frac{r_{n,mk}}{\sqrt{d_{n,m}}}\mathbf{a}_n^{(m)} \quad (49)$$

$$= \mathbf{w}_n^{(k)} - \varphi_{n,1}^{(k)}\left(\mathbf{w}_n^{(k-1)} - \sum_{m=1}^{k-2}\frac{r_{n,m(k-1)}}{\sqrt{d_{n,m}}}\mathbf{a}_n^{(m)}\right) - \sum_{m=1}^{k-2}\frac{r_{n,mk}}{\sqrt{d_{n,m}}}\mathbf{a}_n^{(m)} \quad (50)$$

$$= \mathbf{w}_n^{(k)} - \varphi_{n,1}^{(k)}\mathbf{w}_n^{(k-1)} - \sum_{m=1}^{k-2}\frac{r_{n,mk} - \varphi_{n,1}^{(k)}r_{n,m(k-1)}}{\sqrt{d_{n,m}}}\mathbf{a}_n^{(m)}. \quad (51)$$

Similarly, let

$$\varphi_{n,m}^{(k)} = \frac{1}{\sqrt{d_{n,k-m}}}\left(r_{n,(k-m)k} - \sum_{u=1}^{m-1}\varphi_{n,u}^{(k)}r_{n,(k-m)(k-u)}\right) \quad \text{for } 2 \le m \le k-1.$$

Then we can obtain the result in (20) by repeating the steps from (49) – (51). △△△

APPENDIX D
PROOF OF LEMMA 4

When $\mathbf{H}_n$ is given, the statistics of $[\mathbf{C}_n^{(k)}]_{11}$ and $[\mathbf{P}_n^{(k)}]_{11}$ depends only on $\mathbf{a}_n^{(k)}$. Since $\{\mathbf{w}_n^{(i)}\}_{i=1}^k$ are i.i.d. circularly symmetric complex Gaussian random vectors, using (20) we know that $\mathbf{a}_n^{(k)}|\mathbf{H}_n$ is also a circularly symmetric complex Gaussian random vector with covariance matrix $\left(1 + \sum_{m=1}^{k-1}|\varphi_{n,m}^{(k)}|^2\right)\mathbf{I}_{M_r}$. Because $\mathbf{a}_n^{(k)}|\mathbf{H}_n$ is circularly symmetric complex Gaussian, we have $\mathrm{E}\left[\mathbf{a}_n^{(k)}|\mathbf{H}_n\right] = \mathbf{0}$ and $\mathrm{E}\left[\mathbf{a}_n^{(k)}\mathbf{a}_n^{(k)T}|\mathbf{H}_n\right] = \mathbf{0}$. As a result, we have $\mathrm{E}\left[[\mathbf{C}_n^{(k)}]_{11}|\mathbf{H}_n\right] = 0$ and

$$\begin{aligned}\mathrm{E}\left[[\mathbf{C}_n^{(k)}]_{11}^2|\mathbf{H}_n\right] &= 2\|\mathbf{v}_n^{(k)}\|^2\left(1+\sum_{m=1}^{k-1}|\varphi_{n,m}^{(k)}|^2\right)\\ &= 2d_{n,k}\left(1+\sum_{m=1}^{k-1}|\varphi_{n,m}^{(k)}|^2\right), \qquad (52)\end{aligned}$$

where in the second equality we have used $d_{n,k} = [\mathbf{H}_n^{(k)\dagger}\mathbf{H}_n^{(k)}]_{11} = \|\mathbf{v}_n^{(k)}\|^2$ obtained from (10). Using (19) we can obtain

$$\begin{aligned}\mathrm{E}\left[[\mathbf{P}_n^{(k)}]_{11}|\mathbf{H}_n\right] &= M_r\left(1+\sum_{m=1}^{k-1}|\varphi_{n,m}^{(k)}|^2\right)\\ &\quad -\sum_{l=1}^{k-1}\mathrm{E}\left[|\mathbf{a}_n^{(l)\dagger}\mathbf{v}_n^{(k)}+\mathbf{v}_n^{(l)\dagger}\mathbf{a}_n^{(k)}|^2|\mathbf{H}_n\right]/d_{n,l}. \qquad (53)\end{aligned}$$

As $\{\mathbf{w}_n^{(i)}\}_{i=1}^k$ are circularly symmetric complex Gaussian vectors, using Lemma 3 it can be shown that $\mathrm{E}\left[\mathbf{a}_n^{(k)}\mathbf{a}_n^{(m)T}|\mathbf{H}_n\right] = \mathbf{0}$. Thus the expectation in the second term of (53) can be written as

$$\begin{aligned}&\mathrm{E}\left[|\mathbf{a}_n^{(l)\dagger}\mathbf{v}_n^{(k)}+\mathbf{v}_n^{(l)\dagger}\mathbf{a}_n^{(k)}|^2|\mathbf{H}_n\right]\\ &= d_{n,k}\left(1+\sum_{m=1}^{l-1}|\varphi_{n,m}^{(l)}|^2\right)+d_{n,l}\left(1+\sum_{m=1}^{k-1}|\varphi_{n,m}^{(k)}|^2\right). \qquad (54)\end{aligned}$$

Substituting (54) into (53), we obtain the conditional the mean of $[\mathbf{P}_n^{(k)}]_{11}|\mathbf{H}_n$ in (25). △△△

APPENDIX E
PROOF OF THEOREM 1

Observing (24) and (25), we can see that $\mathrm{E}[b_{n+1,k}|\mathbf{H}_n]$ depends only on $r_{n,ij}$ for $1 \le i \le j \le M_t$. Note that in the QR decomposition of $\mathbf{H}_n$, $\{r_{n,ij}\}_{1\le i\le j\le M_t}$ are independent [34]. As $\{r_{n,ij}\}$ are independent and $r_{n,kk}^2 = (2^{b_{n,k}}-1)/\gamma_k$ is given, we have $\tilde{b}_{n+1,k} = \mathrm{E}\left[b_{n+1,k}|\mathbf{b}_n\right] = \mathrm{E}_{\{r_{n,ij},i<j\}}\left[\mathrm{E}\left[b_{n+1,k}|\mathbf{H}_n\right]\right]$. By taking the expectations of (23) over $r_{n,ij}$ for $i<j$, we have

$$\begin{aligned}&\mathrm{E}\left[b_{n+1,k}|\mathbf{b}_n\right]\\ &= b_{n,k}+\frac{\epsilon^2}{\log_e(2)}\left(\frac{\Omega_n^{(k)}-d_{n,k}}{\gamma_k^{-1}+d_{n,k}}-\frac{\Psi_n^{(k)}}{2(\gamma_k^{-1}+d_{n,k})^2}\right), \qquad (55)\end{aligned}$$

where $\Omega_n^{(k)} = \mathrm{E}_{\{r_{n,ij},i<j\}}\left[\mathrm{E}\left[[\mathbf{P}_n^{(k)}]_{11}|\mathbf{H}_n\right]\right]$ and $\Psi_n^{(k)} = \mathrm{E}_{\{r_{n,ij},i<j\}}\left[\mathrm{E}\left[[\mathbf{C}_n^{(k)}]_{11}^2|\mathbf{H}_n\right]\right]$. Using (24) and (25), we observe that $\Omega_n^{(k)}$ and $\Psi_n^{(k)}$ both depend on $\mathrm{E}_{\{r_{n,ij},i<j\}}\left[1+\sum_{m=1}^{\tau-1}|\varphi_{n,m}^{(\tau)}|^2\right]$ for $1\le\tau\le k$, which turns out to have a closed form, to be proved next.

Using Lemma 3, $\varphi_{n,m}^{(l)}$ is given by

$$\varphi_{n,m}^{(l)} = \frac{1}{\sqrt{d_{n,l-m}}}\left(r_{n,(l-m)l}-\sum_{t=1}^{m-1}\varphi_{n,t}^{(l)}r_{n,(l-m)(l-t)}\right), \quad \text{for } 1\le m\le l-1. \qquad (56)$$

Let $\mathbb{A}(n,m,l)$ be the set $\{\varphi_{n,t}^{(l)}\}_{t=1}^{m-1}$ and $\mathbb{B}(n,m,l) = \{r_{n,(l-m)j}\}_{j=l-m+1}^{l}$. From Lemma 3, we know $\varphi_{n,t}^{(l)}$ in (56) depends on $r_{n,ij}$ for $l-t\le i<j\le l$. As a result, the set $\mathbb{A}(n,m,l)$ depends on $r_{n,ij}$ for $l-m+1\le i<j\le l$. Since $r_{n,ij}$ for $1\le i\le j\le M_t$ are independent random variables, we know that the set $\mathbb{A}(n,m,l)$ is statistically independent of the set $\mathbb{B}(n,m,l)$. Thus, $\mathrm{E}_{\{r_{n,ij},i<j\}}\left[|\varphi_{n,m}^{(l)}|^2\right]$ is given by

$$\begin{aligned}&\mathrm{E}_{\{r_{n,ij},i<j\}}\left[|\varphi_{n,m}^{(l)}|^2\right] = \frac{1}{d_{n,l-m}}\\ &\cdot\left[1+\sum_{t=1}^{m-1}\mathrm{E}_{\{r_{n,ij},i<j\}}\left[|\varphi_{n,t}^{(l)}|^2\right]\right], \quad \text{for } 1\le m\le l-1, \qquad (57)\end{aligned}$$

where we have used the fact that $\{r_{n,ij}\}_{i<j}$ are complex Gaussian random variables with zero mean and unit variance [34]. Applying (57) for the case $m=l-1$, we have

$$\begin{aligned}&\mathrm{E}_{\{r_{n,ij},i<j\}}\left[1+\sum_{m=1}^{l-1}|\varphi_{n,m}^{(l)}|^2\right]\\ &=1+\mathrm{E}_{\{r_{n,ij},i<j\}}\left[\sum_{m=1}^{l-2}|\varphi_{n,m}^{(l)}|^2\right]+\mathrm{E}_{\{r_{n,ij},i<j\}}\left[|\varphi_{n,l-1}^{(l)}|^2\right]\\ &=\left(1+\frac{1}{d_{n,1}}\right)\left(1+\mathrm{E}_{\{r_{n,ij},i<j\}}\left[\sum_{m=1}^{l-2}|\varphi_{n,m}^{(l)}|^2\right]\right).\end{aligned}$$

In a similar manner, we apply (57) for the case $m=\tau-2, m=\tau-3,\ldots,m=1$, then we get

$$\mathrm{E}_{\{r_{n,ij},i<j\}}\left[1+\sum_{m=1}^{\tau-1}|\varphi_{n,m}^{(\tau)}|^2\right] = \prod_{m=1}^{\tau-1}\left(1+\frac{1}{d_{n,m}}\right). \qquad (58)$$

Using the above result, we can obtain $\Omega_n^{(k)} = \mathrm{E}_{\{r_{n,ij},i<j\}}\left[\mathrm{E}\left[[\mathbf{P}_n^{(k)}]_{11}|\mathbf{H}_n\right]\right]$ and $\Psi_n^{(k)} = \mathrm{E}_{\{r_{n,ij},i<j\}}\left[\mathrm{E}\left[[\mathbf{C}_n^{(k)}]_{11}^2|\mathbf{H}_n\right]\right]$, and the theorem follows. △△△

REFERENCES

[1] H. Sampath, P. Stoica, and A. Paulraj, "Generalized linear precoder and decoder design for MIMO channelsusing the weighted MMSE criterion," *IEEE Trans. Commun.*, vol. 49, pp. 2198–2206, Dec. 2001.

[2] A. Scaglione, P. Stoica, S. Barbarossa, G. B. Giannakis, and H. Sampath, "Optimal designs for space-time linear precoders and decoders," *IEEE Trans. Signal Process.*, vol. 50, pp. 1051–1064, May 2002.

[3] Y. Ding, T. N. Davidson, Z.-Q. Luo, and K.-M. Wong, "Minimum BER block precoders for zero-forcing equalization," *IEEE Trans. Signal Process.*, vol. 51, pp. 2410–2423, Sep. 2003.

[4] D. P. Palomar, J. M. Cioffi, and M. A. Lagunas, "Joint Tx-Rx beamforming design for multicarrier MIMO channels: A unified framework for convex optimization," *IEEE Trans. Signal Process.*, vol. 51, pp. 2381–2401, Sep. 2003.

[5] A. J. Goldsmith and S. G. Chua, "Variable-rate variable-power MQAM for fading channels," *IEEE Trans. Commun.*, vol. 45, no. 10, pp. 1218–1230, Oct. 1997.

[6] S. M. Alouini and A. J. Goldsmith, "Adaptive modulation over Nakagami fading channels," *Wireless Pers. Commun.*, vol. 13, no. 1-2, pp. 119–143, May 2000.

[7] P. F. Xia, S. L. Zhou, and G. B. Giannakis, "Adaptive MIMO-OFDM based on partial channel state information," *IEEE Trans. Signal Process.*, vol. 52, no. 1, pp. 202–213, Jan. 2004.

[8] P. Yang, Y. Xiao, L. Li, Q. Tang, Y. Yu, and S. Li, "Link adaptation for spatial modulation with limited feedback," *IEEE Trans. Veh. Technol.*, vol. 61, no. 8, pp. 3808–3813, Oct. 2012.

[9] C.-C. Li, Y.-P. Lin, S.-H. Tsai, and P. P. Vaidyanathan, "Optimization of transceivers with bit allocation to maximize bit rate for MIMO transmission," *IEEE Trans. Commun.*, vol. 57, no. 11, pp. 3556–3560, Dec. 2009.

[10] D. J. Love, R. W. Heath Jr., V. K. N. Lau, D. Gesbert, B. D. Rao, and M. Andrews, "An overview of limited feedback in wireless communication systems," *IEEE Sel. Area Commun.*, vol. 26, no. 8, pp. 1341–1365, Oct. 2008.

[11] D. J. Love and R. W. Heath Jr., "Limited feedback unitary precoding for spatial multiplexing systems," *IEEE Trans. Inf. Theory*, vol. 51, no. 8, pp. 2967–2976, Aug. 2005.

[12] J. C. Rho and B. D. Rao, "Design and analysis of MIMO spatial multiplexing systems with quantized feedback," *IEEE Trans. Signal Process.*, vol. 54, no. 8, pp. 4730–4740, Dec. 2006.

[13] S. Zhou and B. Li, "BER criterion and codebook construction for finite-rate precoded spatial multiplexing with linear receivers," *IEEE Trans. Signal Process.*, vol. 54, no. 5, pp. 1653–1665, May 2006.

[14] W. Santipach and M. L. Honig, "Capacity of a multiple-antenna fading channel with a quantized precoding matrix," *IEEE Trans. Inf. Theory*, vol. 55, no. 3, pp. 1218–1234, Mar. 2009.

[15] Q. Li, X. E. Lin, and J. Zhang, "MIMO precoding in 802.16e WiMAX," *J. Commun. Netw.*, vol. 9, no. 2, pp. 141–149, Jun. 2007.

[16] S. T. Chung, A. Lozano, and H. C. Huang, "Approaching eigenmode BLAST channel capacity using V-BLAST with rate and power feedback," in *Proc. 54th IEEE Veh. Technol. Conf. (VTC)*, 2001, vol. 2, p. 915, 919.

[17] H. Zhuang, L. Dai, S. Zhou, and Y. Yao, "Low complexity per-antenna rate and power control approach for closed-loop V-BLAST," *IEEE Trans. Commun.*, vol. 51, no. 11, pp. 1783–1787, Nov. 2003.

[18] Y.-P. Lin, H.-C. Chen, and P. Jeng, "Bit allocation and statistical precoding for correlated MIMO channels with limited feedback," *IEEE Trans. Veh. Technol.*, vol. 61, no. 2, pp. 597–606, Feb. 2012.

[19] B. E. Godana and T. Ekman, "Parametrization based limited feedback design for correlated MIMO channels using new statistical models," *IEEE Trans. Wireless Commun.*, vol. 12, no. 10, pp. 5172–5184, Oct. 2013.

[20] D. Sacristán-Murga and A. Pascual-Iserte, "Differential feedback of MIMO channel Gram matrices based on geodesic Curves," *IEEE Trans. Wireless Commun.*, vol. 9, no. 12, pp. 3714–3727, Dec. 2010.

[21] K. Huang, R. W. Heath Jr., and J. G. Andrews, "Limited feedback beamforming over temporally-correlated channels," *IEEE Trans. Signal Process.*, vol. 57, no. 5, pp. 1959–1975, May 2009.

[22] R. Etkin and D. N. C. Tse, "Degrees of freedom in some underspread MIMO fading channels," *IEEE Trans. Inf. Theory*, vol. 52, no. 4, pp. 1576–1608, Apr. 2006.

[23] T. Kim, D. J. Love, and B. Clerckx, "MIMO systems with limited rate differential feedback in slowly varying channels," *IEEE Trans. Commun.*, vol. 59, no. 4, pp. 1175–1189, Apr. 2011.

[24] L. Zhang, L. Song, M. Ma, and B. Jiao, "On the minimum differential feedback for time-correlated MIMO Rayleigh block-fading channels," *IEEE Trans. Commun.*, vol. 60, no. 2, pp. 411–420, Feb. 2012.

[25] J. Choi, B. Clerckx, N. Lee, and G. Kim, "A new design of polar-cap differential codebook for temporally/spatially correlated MISO channels," *IEEE Trans. Wireless Commun.*, vol. 11, no. 2, pp. 703–711, Feb. 2012.

[26] Y.-P. Lin, "Variable-rate transmission for MIMO time-correlated channels with limited feedback," *IEEE Trans. Signal Process.*, vol. 62, no. 19, pp. 5085–5094, 2014.

[27] J. G. Proakis, *Digital Communication*, 4th ed. New York, NY, USA: McGraw-Hill, 2000.

[28] C. C. Weng, C. Y. Chen, and P. P. Vaidyanathan, "MIMO transceivers with decision feedback and bit loading: Theory and optimization," *IEEE Trans. Signal Process.*, vol. 58, no. 3, pp. 1334–1346, Mar. 2010.

[29] J. S. Chow, J. C. Tu, and J. M. Cioffi, "A discrete multitone transceiver system for HDSL applications," *IEEE J. Sel. Areas Commun.*, pp. 895–908, Aug. 1991.

[30] G. D. Dudevoir, J. S. Chow, S. Kasturia, and J. M. Cioffi, "Vector coding for T1 transmission in the ISDN digital subscriber loop," in *Proc. IEEE Int. Conf. Commun.*, Jun. 1989, pp. 536–540.

[31] K. Sayood*, Introduction to Data Compression*, 3rd ed. : Morgan Kaufmann, 2006.

[32] G. H. Golub and C. F. Van Loan*, Matrix Computations*, 3rd ed. Baltimore, MD, USA: Johns Hopkins Univ. Press, 1996.

[33] S. M. Kay*, Fundamentals of Statistical Signal Processing: Estimation Theory*. Upper Saddle River, NJ, USA: Prentice-Hall, 1993, vol. 1.

[34] A. K. Gupta and D. K. Nagar*, Matirx Variate Distributions*. London, U.K.: Chapman & Hall/CRC, 1999.

[35] "Guidelines for evaluation of radio interface technologies for IMT-advanced," ITU-R, Rep. ITU-R M.2135-1, 2009.

[36] P. W. Wolniansky, G. J. Foschini, G. D. Golden, and R. A. Valenzuela, "V-BLAST: An architecture for realizing very high data rates over the rich-scattering wireless channel," in *Proc. URSI Int. Symp. Signals, Syst., Electron.*, 1998, pp. 295–300.

[37] Y.-P. Lin and S.-M. Phoong, "Statistical bit allocation and statistical precoding for correlated MIMO channels with decision feedback," *IEEE Signal Process. Lett.*, vol. 19, no. 11, pp. 761–764, Nov. 2012.

[38] G. D. Forney Jr. and M. V. Eyuboglu, "Combined equalization and coding using precoding," *IEEE Commun. Mag.*, vol. 29, no. 12, pp. 25–34, Dec. 1991.

[39] G. L. Stüber*, Principles of Mobile Communication*. New York, NY, USA: Springer, 2000.

Chien-Chang Li was born in Penghu, Taiwan, 1980. He received the B.S. degree in power mechanical engineering from the National Tsing-Hua University, Taiwan in 2003 and Ph.D. degrees in electrical engineering from the National Chiao Tung University, Taiwan in 2010. He worked as a Postdoctoral Researcher in the department of electrical engineering, National Chiao Tung University, Taiwan in 2010–2013. He is currently a senior engineer in Office of Chief Technology Officer, MediaTek Inc. His research interests mainly include digital signal processing, multirate filter banks, and wireless communications.

Yuan-Pei Lin (S'93–M'97–SM'03) was born in Taipei, Taiwan, 1970. She received the B.S. degree in control engineering from the National Chiao-Tung University, Taiwan, in 1992, and the M.S. degree and the Ph.D. degree, both in electrical engineering from California Institute of Technology, in 1993 and 1997, respectively. She joined the Department of Electrical and Control Engineering of National Chiao-Tung University, Taiwan, in 1997. Her research interests include digital signal processing, multirate filter banks, and signal processing for digital communications.

She was a recipient of Ta-You Wu Memorial Award in 2004. She served as an associate editor for IEEE TRANSACTION ON SIGNAL PROCESSING, IEEE TRANSACTION ON CIRCUITS AND SYSTEMS II, IEEE SIGNAL PROCESSING LETTERS, IEEE TRANSACTION ON CIRCUITS AND SYSTEMS I, *EURASIP Journal on Applied Signal Processing*, and *Multidimensional Systems and Signal Processing*, Academic Press. She was a Distinguished Lecturer of the IEEE Circuits and Systems Society for 2006–2007. She has also coauthored two books, Signal Processing and Optimization for Transceiver Systems, and Filter Bank Transceivers for OFDM and DMT Systems, both by Cambridge University Press, 2010